S1 – Supplemental graphics and results

Table S1: T_{max} calibration values (shown in Fig. S13).

Compound	Saturation pressure (Pa)	Measured T_{max} values (˚C)
PEG-5	$(5.29 \pm 0.65) \times 10^{-4}$	27.1 ± 0.9
PEG-6	$(3.05 \pm 0.49) \times 10^{-5}$	54 ± 3.8
PEG-7	$(1.29 \pm 0.35) \times 10^{-6}$	73.9 ± 3.3
PEG-8	$(9.2 \pm 6.4) \times 10^{-8}$	89.2 ± 3.3

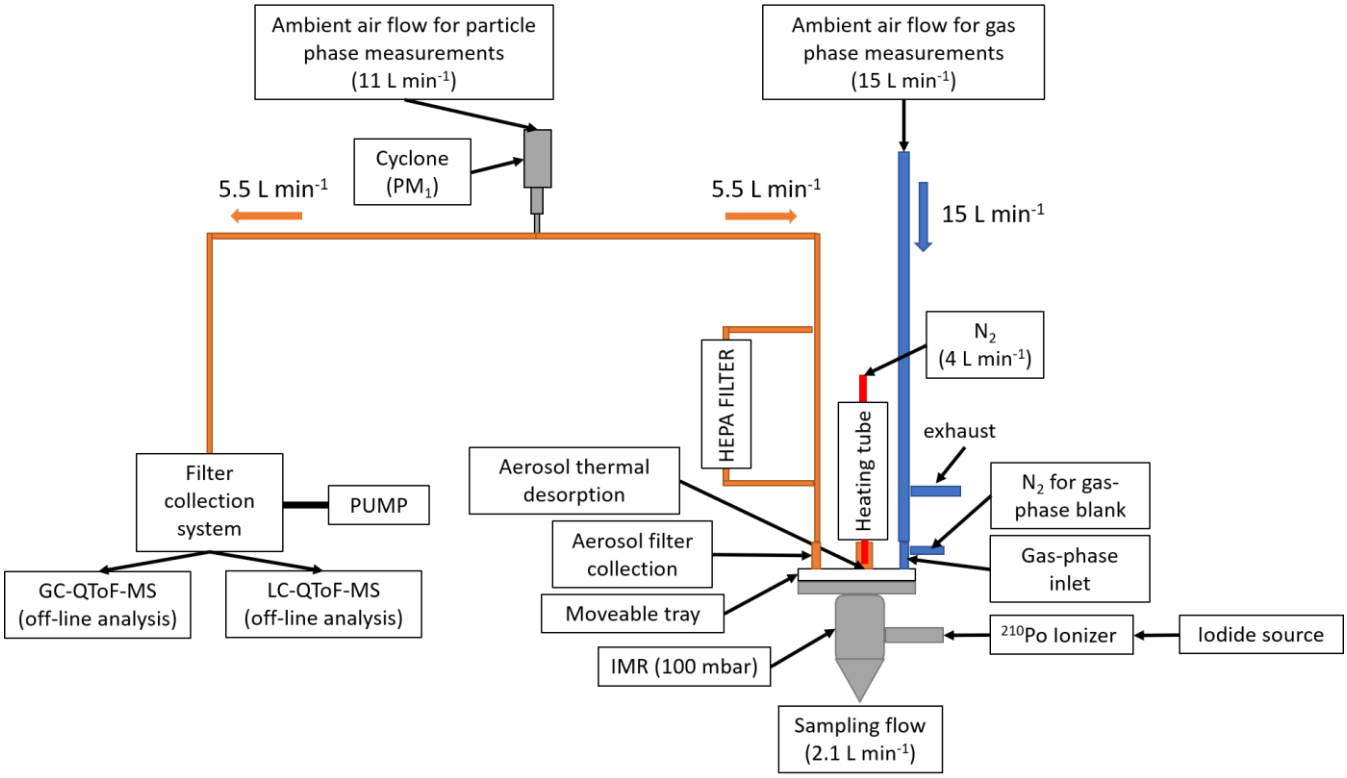

Figure S1: Measurement setup used in this study. The orange lines correspond to the sampling lines for the particle phase measurements, while blue lines correspond to the gas phase sampling.

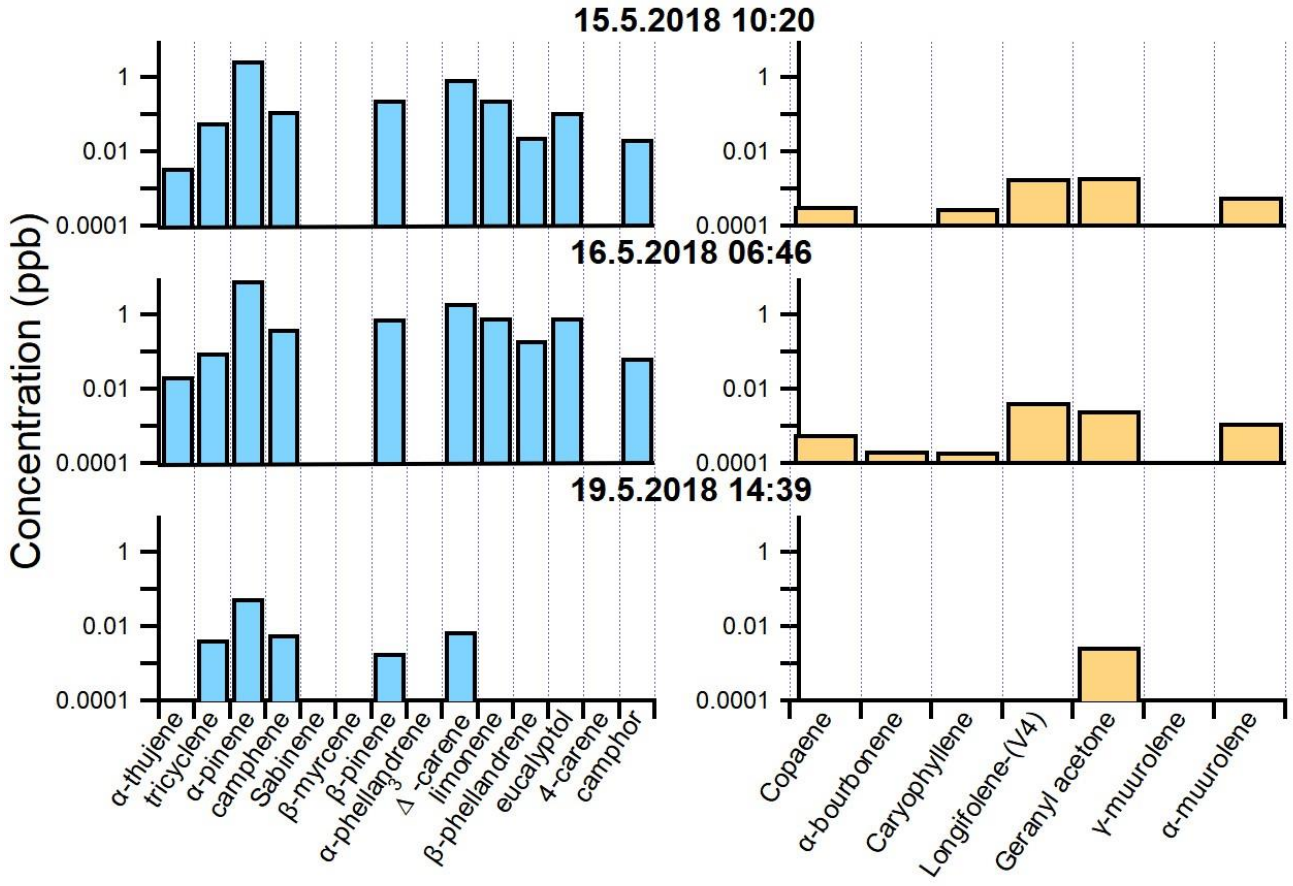

Figure S2: Monoterpene (left) and sesquiterpene (right) compounds identified by GC-MS analysis of sorbent tube samples collected for 30 min close to the three events described in this study. The C_{13} oxygenated hydrocarbon geranyl acetone was included in the sesquiterpene graphics.

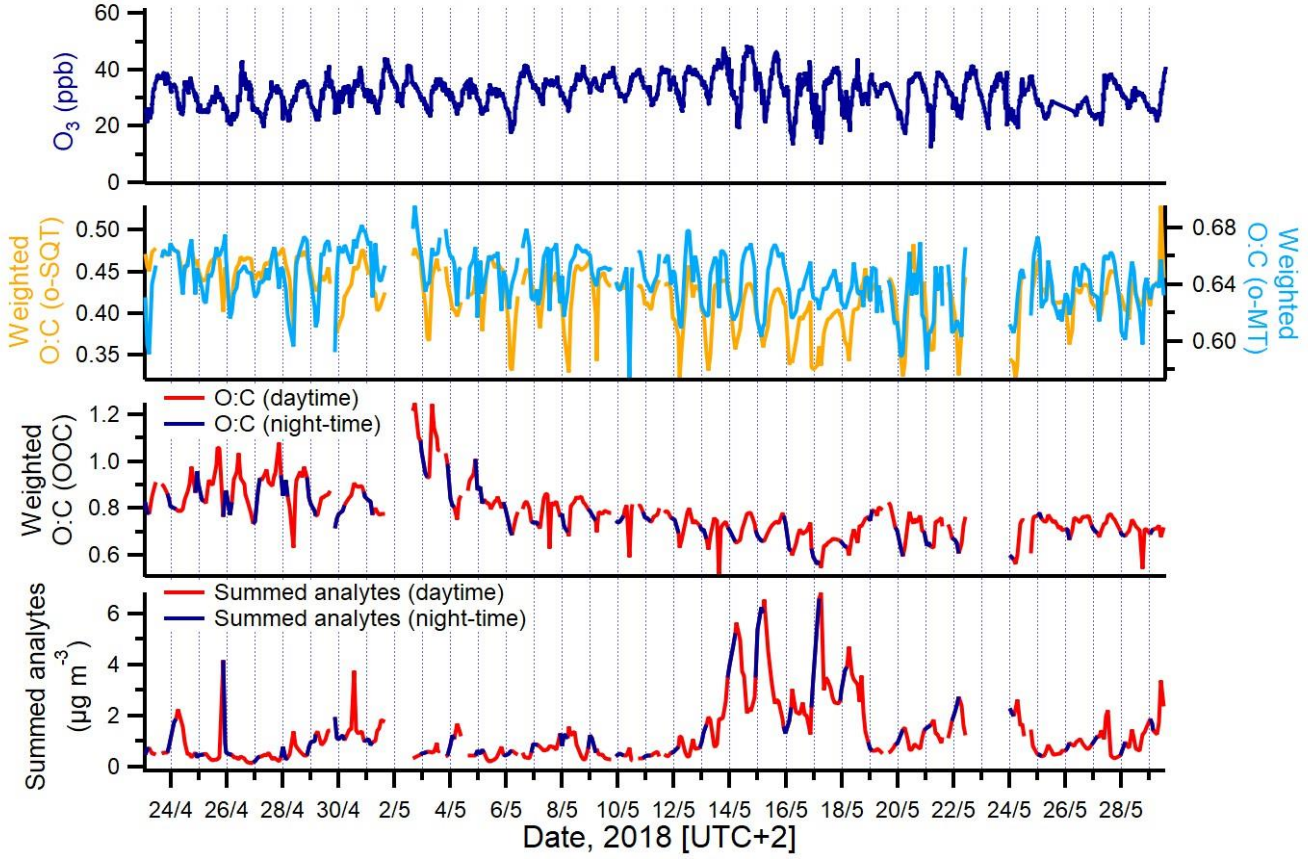

Figure S3: Variation of particle mass concentration (summed analytes) measured by FIGAERO-CIMS, concentration-weighted O:C ratio for oxygenated organic constituents (OOC) in particle phase and for particle analytes attributed to monoterpene (o-MT) or sesquiterpene (o-SQT) oxidation, and ozone mixing ratios, for the full campaign period (cf. Fig. 2).

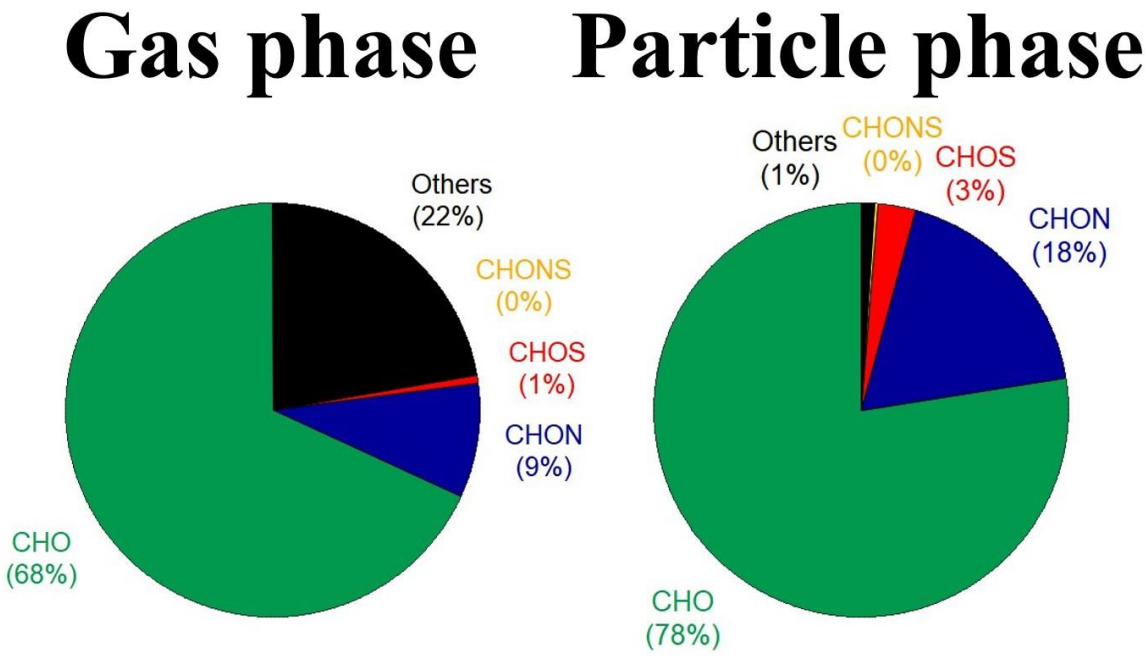

Figure S4: Relative contribution of different analyte classes (CHO, CHON, CHOS, CHONS and Others) measured by FIGAERO-CIMS based on a campaign-wide average.

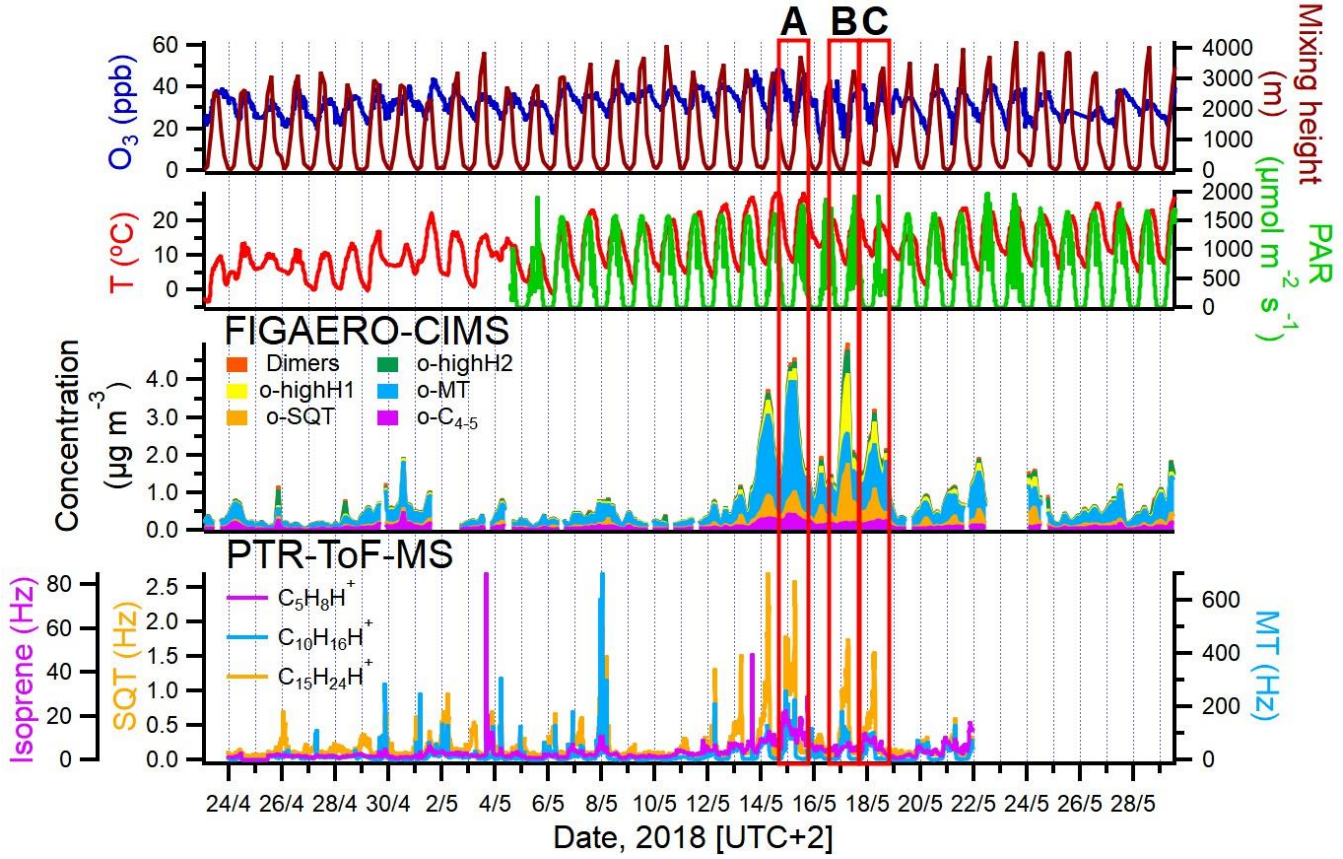

25 **Figure S5: Amounts of monoterpenes, sesquiterpenes and isoprene measured by PTR-ToF-MS (bottom), concentration of sesquiterpene and monoterpene oxidation products (o-SQT and o-MT) measured by FIGAERO-CIMS (middle), and meteorological parameters (temperature and PAR), mixing height and ozone mixing ratios (top) at the sampling site during the full campaign period. The m/z 69, 137 and 205 were used as proxies for isoprene, monoterpenes, and sesquiterpenes, respectively. Note the different axes for isoprene, sesquiterpenes and monoterpenes.**

30

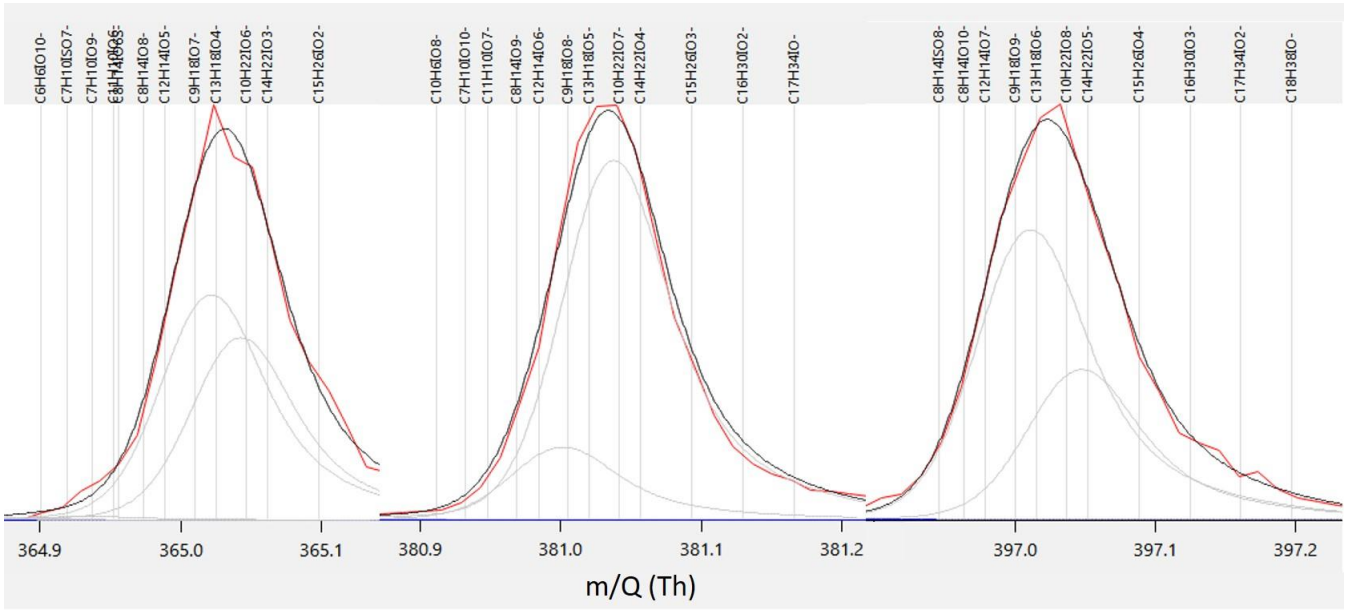

Figure S6: Example of the large number of molecular formulas, given instrumental mass resolving power, possibly contributing to a measured signal in natural samples of atmospheric aerosol particles measured by FIGAERO-CIMS (note that each panel corresponds to a different m/z).

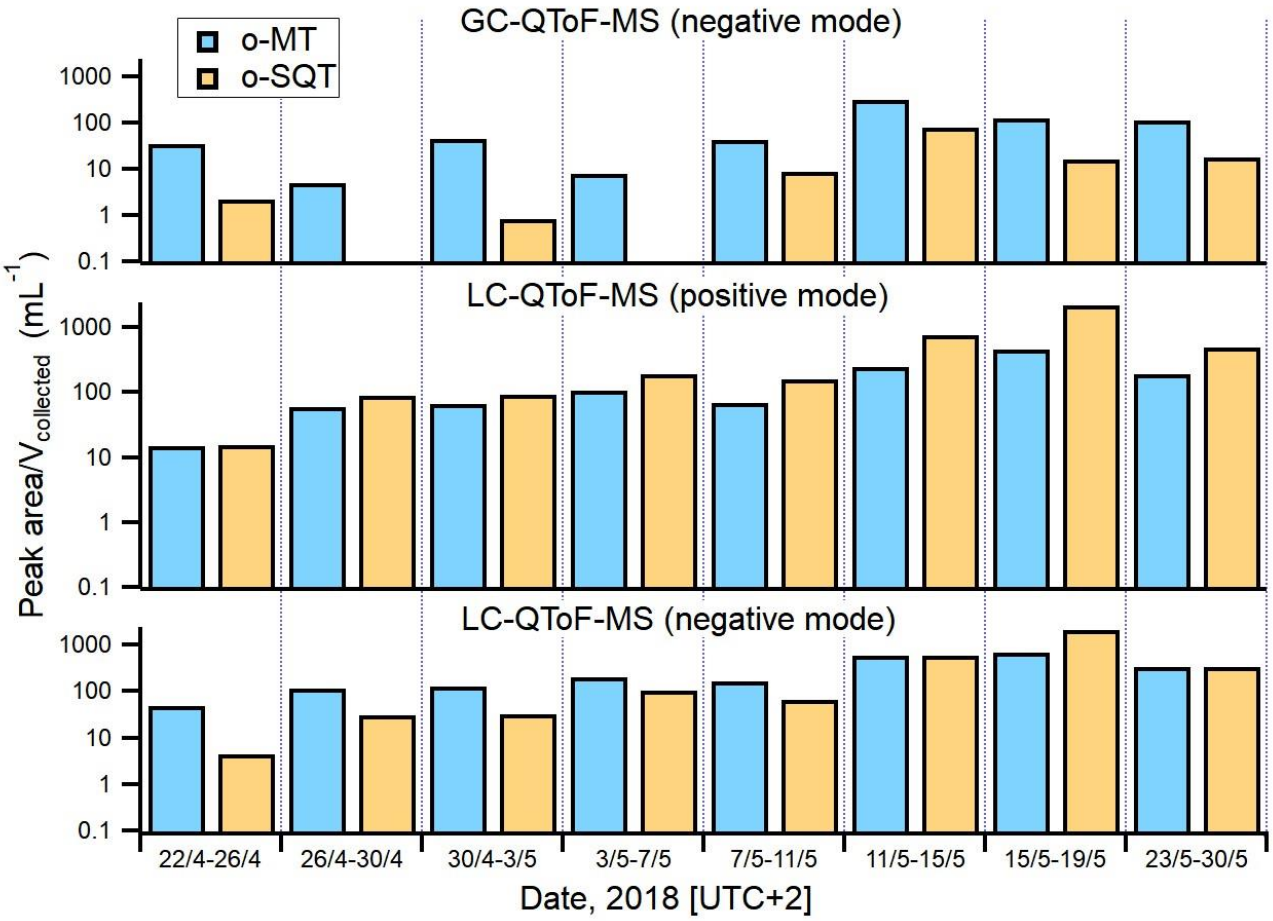

Figure S7: Amounts of monoterpene and sesquiterpene oxidation products (o-MT and o-SQT, normalized by the volume collected) measured by GC-QToF-MS (negative mode) and LC-QToF-MS (positive and negative mode).

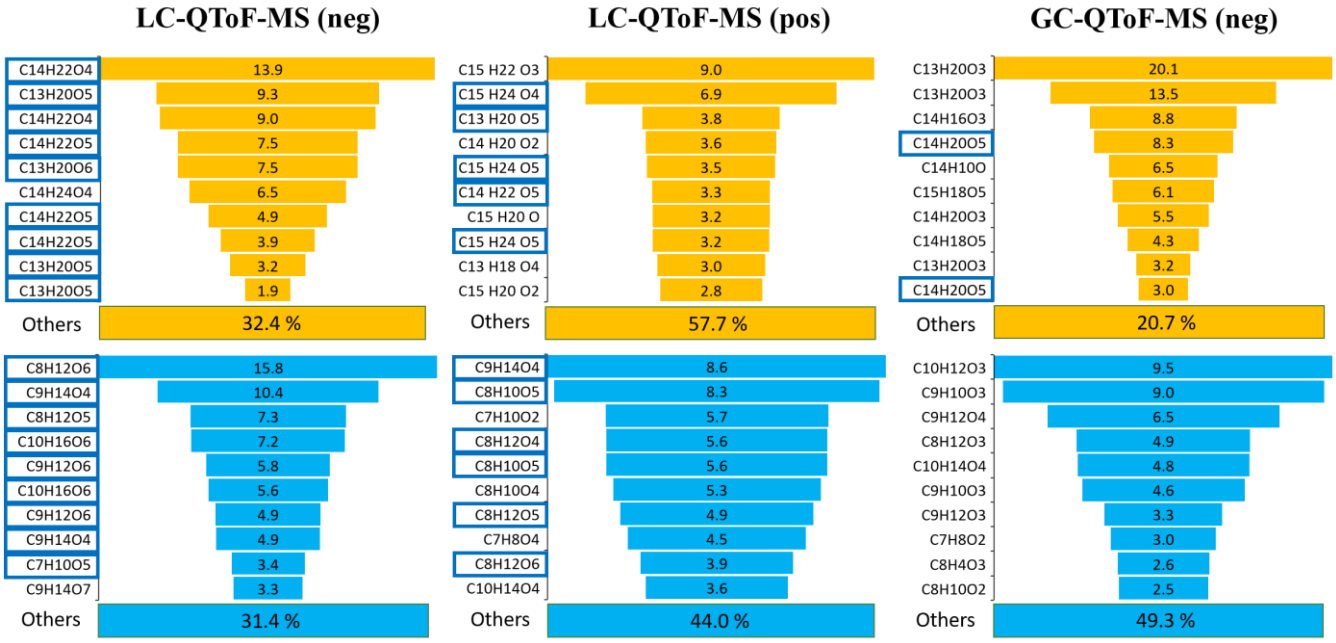

Figure S8: Mass percentage of o-SQT from total o-SQT (upper row) and of o-MT from total o-MT (lower row), based on LC-QToF-MS results (left and center plots for negative and positive polarities, respectively) and GC-QToF-MS results (right plots), during the period between 11.5-15.5 when event A occurred. Blue boxes indicate chemical formulas that were also identified among the 10 most abundant o-SQT and o-MT in FIGAERO-CIMS measurements during event A. The percentages below each of the six sub-plots indicate the mass-based contribution of the remaining o-SQT and o-MT analytes.

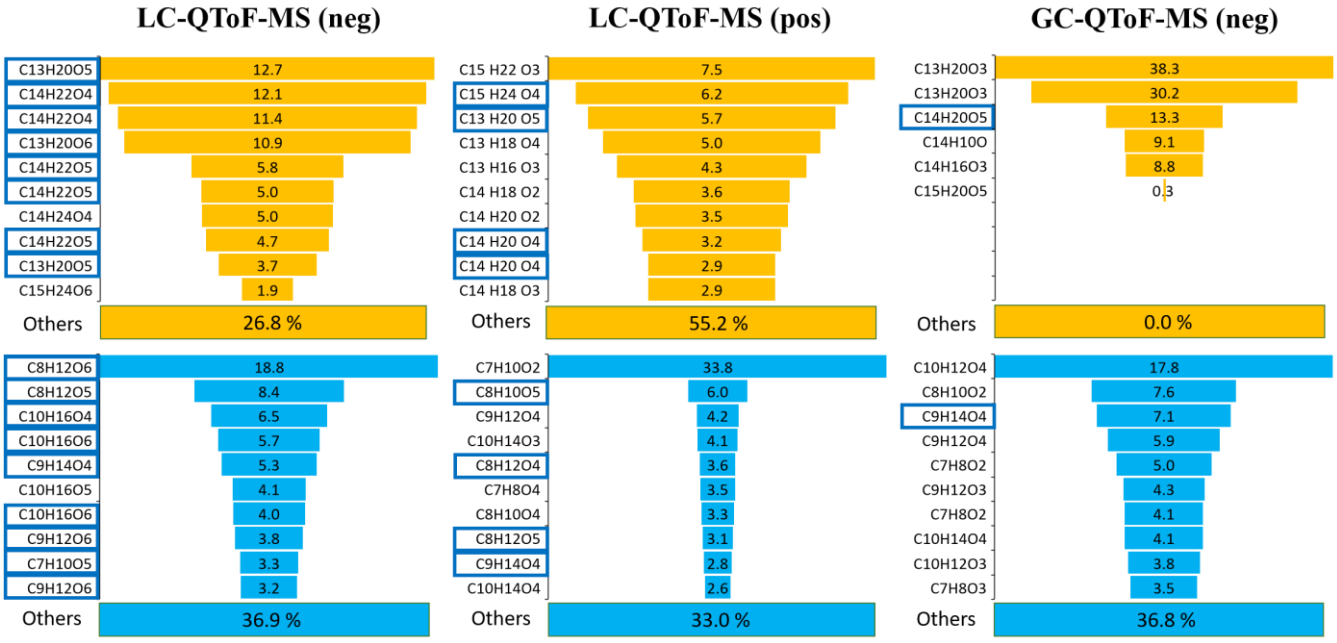

Figure S9: Mass percentage of o-SQT from total o-SQT (upper row) and of o-MT from total o-MT (lower row), based on LC-QToF-MS results (left and center plots for negative and positive polarities, respectively) and GC-QToF-MS results (right plots), during the period between 15.5-19.5 when event B occurred. Blue boxes indicate chemical formulas that were also identified among the 10 most abundant o-SQT and o-MT in FIGAERO-CIMS measurements during event B. The percentages below each of the six sub-plots indicate the mass-based contribution of the remaining o-SQT and o-MT analytes.

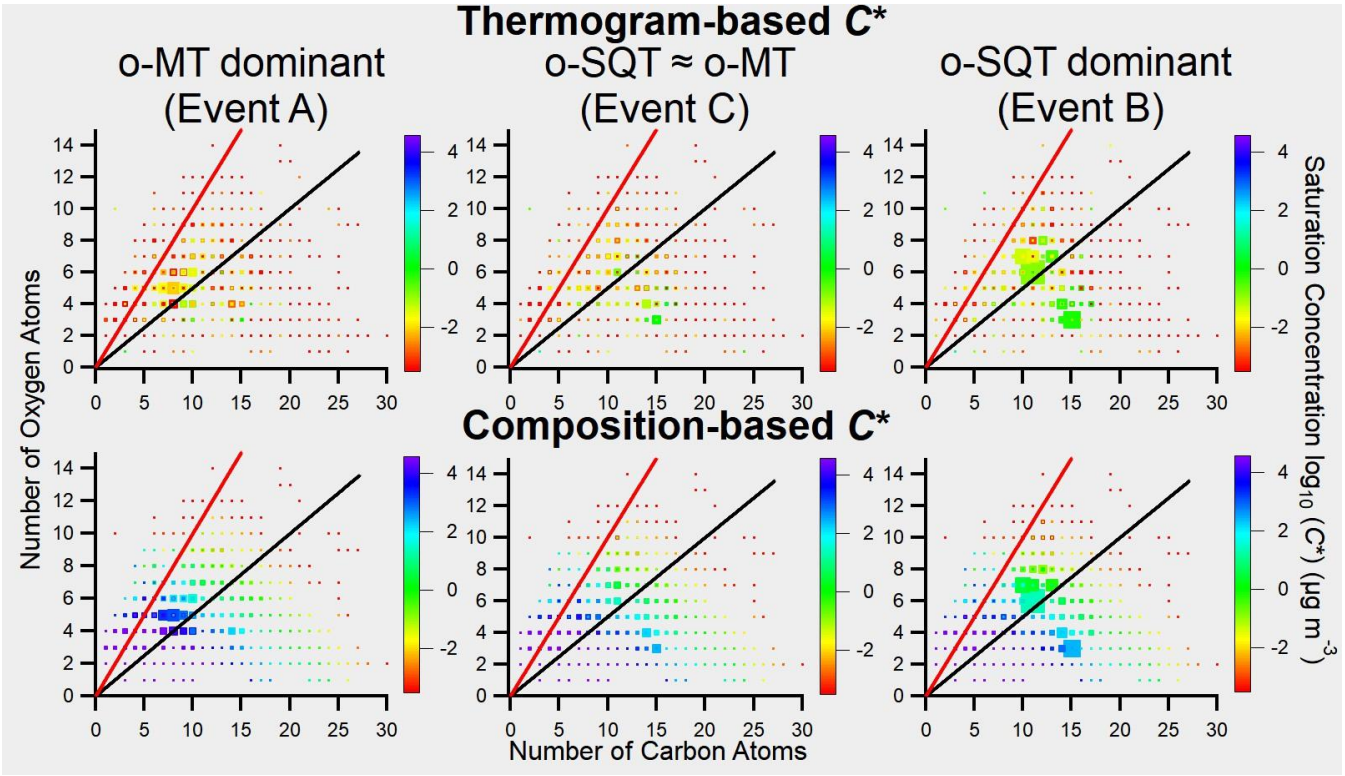

Figure S10: Number of oxygen atoms versus number of carbon atoms for each chemical formula and each studied event. Colors correspond to the saturation concentration *C as derived from the measured T_{max} (upper row) or composition (lower row). The size of a marker corresponds to the concentration of the compounds. The black and red lines in the figures correspond to O:C = 0.5 and O:C = 1 ratios, respectively, for reference. All analytes above LOD (including organonitrates and excluding reagent ions) were included in the graphic.**

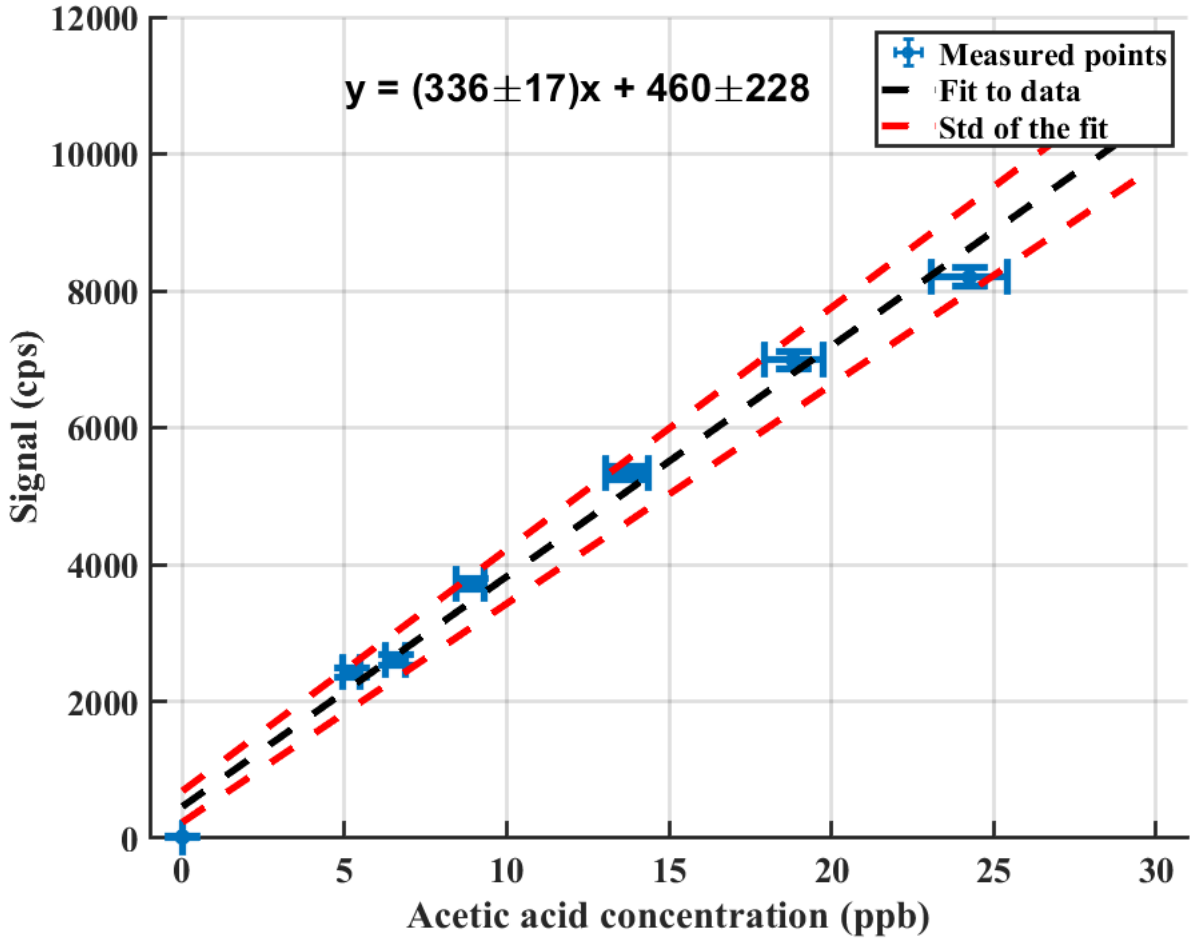

Figure S11: Calibration curve obtained for FIGAERO-CIMS gas phase measurements using acetic acid as calibrant. The acetic acid was prepared in a permeation tube and permeating gas was subsequently diluted with a nitrogen flow to obtain different concentrations. The concentration errors were calculated with propagation of error, while signal errors were estimated from STD + poisson counting error.

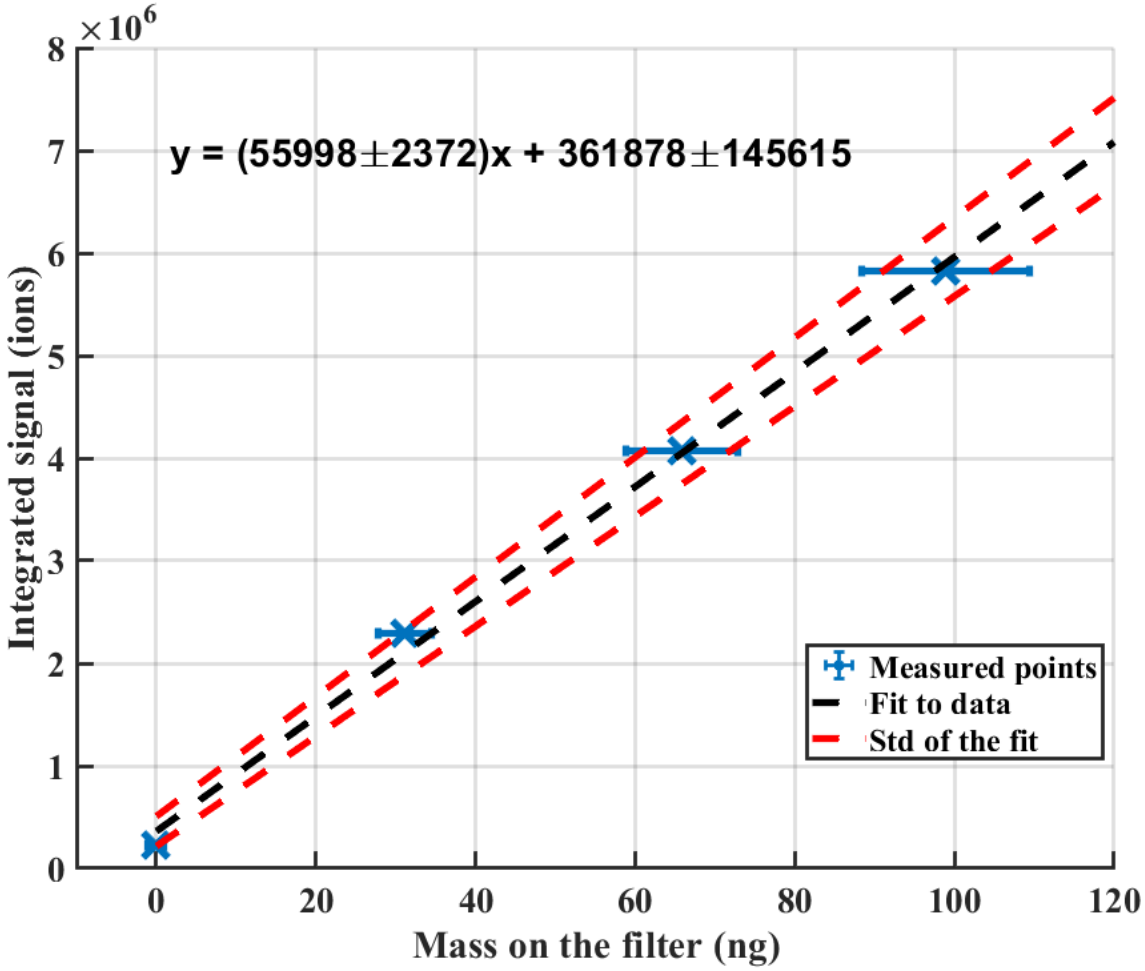

Figure S12: Calibration curve obtained for FIGAERO-CIMS particle phase measurements using a glutaric acid solution (~10 g L^{-1}) prepared in ultrapure water. The solution was then atomized and different aerosol particle mass loadings were collected on the FIGAERO filter and subsequently analyzed by FIGAERO-CIMS, using the same desorption protocol as for the ambient measurements. The concentration errors were calculated with propagation of error, while signal errors were estimated from STD + poisson counting error.

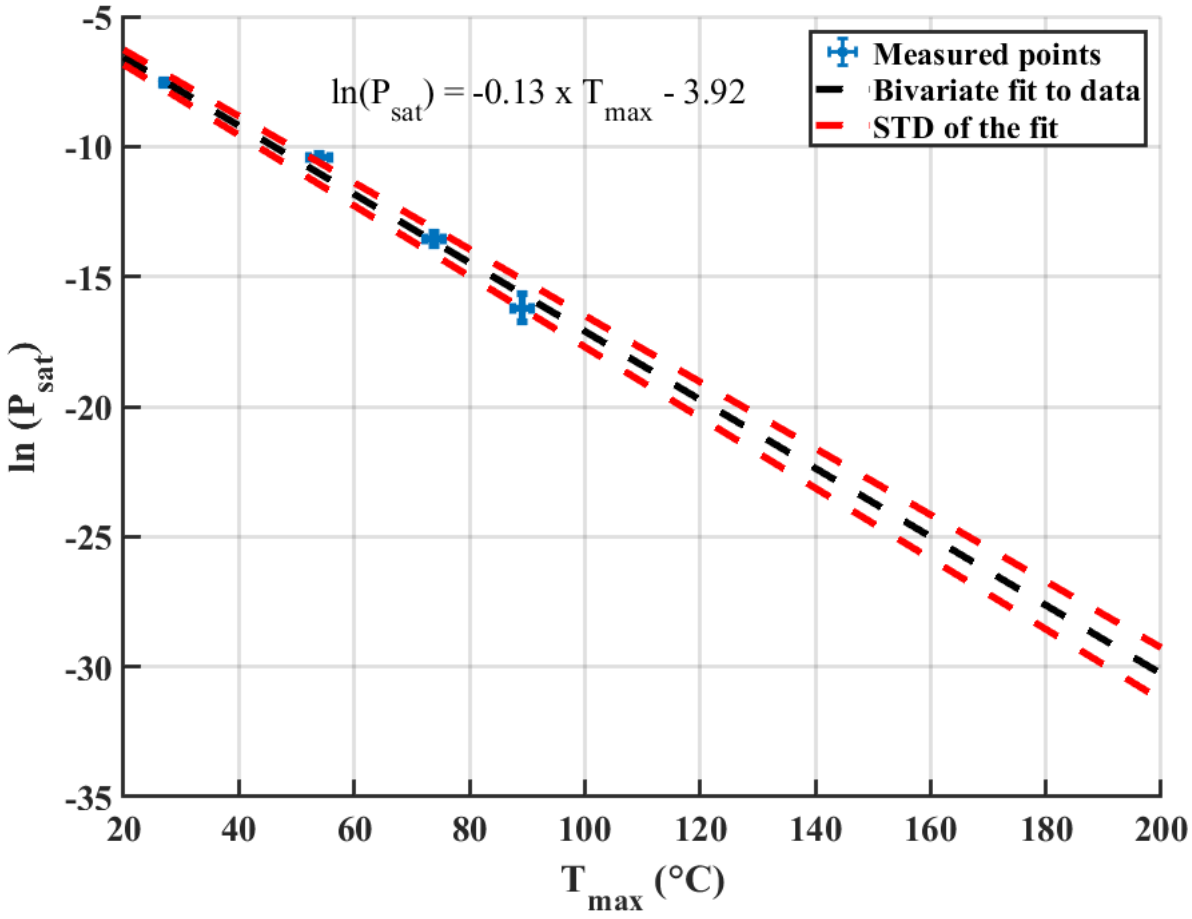

Figure S13: T_{max} calibration curve. The markers show the measured points, the black line shows the applied fit, and the red lines shows the standard deviation of the fit. Bivariate fitting was used to account for uncertainties in both axes.

S2 – Processing of FIGAERO-CIMS data

The data processing was performed using the version 2.5.11 of the Tofware software (Aerodyne Research Inc. and Tofwerk AG) running in Igor Pro (Wavemetrics Inc., USA). This data processing included the optimization of the instrument functions, a mass calibration using the custom peak shape, and a manual creation of a peak list of molecular formulas tentatively identified based on exact masses for the fitting of the HR data. The resolution of the instrument was between 3000 and 5000. The processed data was normalized to the sum of main reagent ions signal (I^- + $I(H_2O)^-$). Gas phase samples were averaged for each measurement cycle of 45 minutes, but the first 17.5 minutes of each gas phase cycle were removed due to carry-over from particle phase measurements. The values for gas phase blank subtraction were obtained by removing the first 17.5 minutes as for the gas phase samples and choosing the second and third (1Hz) point of each blank measurement, in order to take into account the carry-over from the previous gas phase sample and possible interferences from wall adsorptions. The remaining gas phase blank values corresponding to each gas phase cycle were then averaged and subtracted from the sample signal. However, samples were collected at ambient relative humidity, while blanks were performed using dry N_2. The water vapor pressure is known to influence the instrument sensitivity to organic aerosol constituents (e.g. Lee et al., 2014). This may impact on the quantitative measurement of those analytes. Since in Lee et al. (2014) most of few studied organics have exhibited either a negative or negligible dependence on water pressure, it is likely that a small underestimation of gas phase concentrations has occurred in our study. Due to difficulties in estimating the dependence of all measured analytes on the water vapor pressure, results may be considered as semi-quantitative. Similarly, possible imperfections in the zeroing air can also result in increased responses for measured analytes in blank measurements. For the particle phase measurements, the data was averaged to a 20 s time resolution in order to reduce the processing time and smooth the otherwise noisy data. For obtaining amounts desorbing from the filter, the signal (ions s^{-1}) for each chemical formula was integrated over time (s) covering a full desorption cycle. The particle phase blank measurement obtained before and after each sample were averaged, and the values were used for subtracting from the sample signal.

S3 – Complementary information concerning LC-QToF-MS, GC-QToF-MS, and GC-MS analysis

The LC-QToF-MS analysis was performed using reversed phase (RP) chromatography. A Zorbax Eclipse XDB-C18 column (100 × 2.1 mm, 1.8 µm, Agilent Technologies, Palo Alto, CA, USA) was used. The temperature of the column was kept at 50 °C, and the flow rates of mobile phases were set as 0.4 mL min^{-1}. The mobile phases consisted of water (eluent A) and methanol (eluent B), both containing 0.01 % (v/v) of formic acid. The gradient profile employed was as follows: 2 → 100 % B (0–10 min); 100 % B (10–14.5 min); 100 → 2 % B (14.5–14.51 min); 2 % B (14.51–16.50 min). The injection volume in RP was 2 µl. The MS ion source conditions consisted of an ESI source, operated both in positive and negative ionization modes. The drying gas temperature was 325 °C with a flow of 10 L min^{-1}, while sheath gas temperature was 350 °C with a flow of 11 L min^{-1}. The nebulizer pressure was 45 psi, the capillary voltage was 3500 V, and the nozzle voltage was 1000 V. The fragmentor voltage and skimmer were set to 100 V and 45 V, respectively. For data acquisition, the mass range was 20–

1600 amu with an acquisition rate of 1.67 spectra s^{-1}. A continuous mass axis calibration was performed by monitoring two reference ions from an infusion solution throughout the runs. In positive mode the reference ions were m/z 121.050873 and m/z 922.009798, and in negative mode were m/z 112.985587 and m/z 966.000725. The data was pre-processed using the MassHunter Qualitative Analysis software (Agilent Technologies, B.05.00), where the ions were extracted utilizing the "Find by molecular feature" algorithm. The Mass Profiler Professional software (MPP 2.2, Agilent Technologies) was used for compound alignment and posterior data pre-processing. In order to reduce noise and remove insignificant analyte features, only features which had higher signals in the samples than in the blank filter measurements were considered in this study.

For GC-QToF-MS, the GC separation was performed using a HP-5 MS capillary column (Agilent Technologies, Santa Clara, CA) with 30 m × 0.25 mm i.d. and a film thickness of 0.25 µm. The injection volume was 1 µl. The injector was operated at 300 °C. Nitrogen (purity >99.999 %), at a constant flow of 1.2 mL min^{-1}, was used as a carrier gas. The GC oven temperature was as follows: 40 °C (held for 2 min), then 10 °C min^{-1} to 300 °C (held for 5 min), resulting in a total run time of 33 min. The transfer line temperature was 300 °C, while the ion source was kept at 250 °C. The ToF for MS was operated at 10 spectra s^{-1} acquiring the mass range of 50−900 m/z. Methane was used as chemical ionization gas. Emission and electron energy were respectively fixed at 50 µA and 250 eV. The data was exported using the Agilent MassHunter qualitative analysis software (version B.06; Agilent), and pre-processed with the open-source software MZmine 2 (http://mzmine.github.io) for peak detection, peak alignment and peak area normalization.

S4 – Complementary information concerning FIGAERO-CIMS calibration

The CIMS mass calibration was performed using 5 ion masses, namely I^-, $I(H_2O)^-$, $CH_2O_2^-$, I_2^-, and I_3^-. They span the mass range covering most ions of analytical interest. Occasionally, the mass calibration failed due to the presence of a higher intensity peak close to I_3^-. For those periods, a contaminant peak (m/z 339.9840) was used for the mass calibration.

The instrument response function was obtained for both gas and particle phase measurement modes. Glutaric acid (≥ 99 %) and acetic acid (≥ 99.8 %) from Sigma-Aldrich (St. Louis, USA) were used as authentic standards for calibration purposes. For gas phase calibration, a permeation tube containing acetic acid was prepared by weighting the tube on different days and determining the amount of compound loss per time at ambient temperature. The obtained permeation rate was 154 ± 7 ng min^{-1}. The calibration gas was diluted with a nitrogen flow to obtain different concentrations. A linear 7-point (0-24 ppb) calibration curve was obtained (see. Fig. S11). The limit of quantitation (LOQ) for gas phase measurements was determined by averaging, for each sample cycle, the signal (ions s^{-1}) obtained for 15 masses randomly chosen from 800-1000 Th and multiplying the obtained values by a factor of 10. Generally, since no significant contribution to the overall signal is expected from this mass range, the values can be used as an estimate for the instrument noise. All ions that were below the LOQ during the entire campaign period were not considered for this study.

For particle phase calibrations, a stock solution of glutaric acid was prepared in ultrapure water (DirectQ-UV, Milipore, USA) and subsequently diluted with the same solvent to obtain a concentration of ~10 g L^{-1}. The diluted solution was inserted in an

atomizer and different aerosol particle mass loadings were collected on the PTFE filter of the FIGAERO inlet and subsequently analyzed by FIGAERO-CIMS, using the same desorption protocol as during the ambient measurements. The collected mass was derived from the particle concentration monitored with a SMPS (TSI model 3082 coupled with TSI model 3775 CPC) and the response function was obtained. A linear 4-point (0-95 ng) calibration curve was obtained (Fig. S12). The LOQ was calculated with the same method used for the gas phase measurement mode, but by using the average of the values obtained from the integration of signal (ions s^{-1}) over the full desorption duration (s).

The thermogram based volatility calibration was done by atomizing series of polyethylene glycol (PEG) compounds (namely PEG-5, PEG-6, PEG-7 and PEG-8) in an acetonitrile (Fisher Scientific, 99.8% purity) solution as described in Ylisirniö et al. (2020). The solution concentration of each PEG-compound was ~0.5 g L^{-1} at the start of the atomization. Output of the atomizer was monitored with SMPS (TSI model 3082 coupled with TSI model 3775 CPC) and ~100 ng of atomized particles were collected on the FIGAERO filter. Calibration values are shown in Table S1. and calibration line is shown in Fig. S13. The saturation pressure values for PEGs were taken from Krieger et al. (2018). The T_{max} values are averages of three measurements.

S5 - Uncertainties associated with High-Resolution Time-of-Flight Chemical Ionization Mass Spectrometry measurements (HR-ToF-CIMS)

HR-ToF-CIMS (abbreviated in this article as CIMS) is a state-of-art analytical technique that allows the measurement of various classes of oxygenated VOCs and inorganic compounds with good linearity and reproducibility, minimal sample preparation, high sensitivity and selectivity, and high time-resolution (Lee et al., 2014). However, this technique is also prone to some associated errors. One of the main sources of errors is related to the complexity of the ambient samples, combined with limited m/z resolving power and (although less problematically) mass accuracy. Atmospheric gas and particle phase composition is complex, not constant, and involves a diversity of analytes, some of which may only be present during short, specific periods of time out of a measurement campaign spanning many weeks. In many instances, multiple conceivable compositions may underlie a single peak in the mass spectrum (e.g., Fig. S6). As a result, the identification of chemical formulas itself is often highly prone to human error (by e.g. attribution of the wrong molecular formula).

The limited resolution of CIMS might have caused the misidentification of measured chemical formulas with ambiguities in peak fitting (see Sect. 3.2). The limited resolution is particularly critical for higher m/z ions due to the increased peak broadening and complexity of analytes elemental composition. For example, the distribution of measured signal between $C_{10}H_{22}O_7$ and $C_{14}H_{22}O_4$ (see Fig. S6) is challenging considering the proximity of their exact masses. Even though other techniques with higher resolution were also used in this study (LQ-QToF-MS and GC-QToF-MS), those techniques relied on off-line analysis that is also prone for sample losses/modification and cannot provide the same time resolution.

Another limitation of the measurements performed in this study was the unavailability of internal standards. The constant measurement of a known concentration of an internal standard improves the reliability and precision of quantitative measurements since they correct possible errors associated to e.g. analyte losses during sample collection or fluctuations in

instrument sensitivity over time. In theory, the internal standard should be measured at atmospherically relevant concentrations and must be structurally similar to the analytes being measured. However, these requirements are challenging when measuring several analytes present at different concentrations and in particular with the panoply of chemical structures inherent to SOA chemistry. For that reason, the development of a standard mixture that could be used for a reliable quantitation of commonly measured atmospheric compounds would allow to improve the quantitative CIMS measurements. The calibrants and reagent ion sources must also be kept at constant temperature, since permeation tube analyte emission rates are highly dependent on temperature.

Additional errors may occur during the mass calibration and peak fitting procedures. For the CIMS measurements performed in this work, a practical issue for mass calibration was related with the fact that the highest m/z of the calibrants used in this study was 381 (corresponding to I_3^-), but a natural candidate for higher m/z is missing. The identification of an internal standard that allows to cover the full mass range of studied analytes would help in improving the reliability of CIMS analysis for all mass spectra. The presence of analytes at the same nominal mass of calibrants can also affect the calibration, due to software limitations. That was the case in our study where, occasionally, the mass calibration failed due to the presence of a higher intensity peak close to I_3^- (although clearly separated, but at nominal m/z 381; see Sect. S4). For those periods, a contaminant peak (m/z 339.9840) was used for the mass calibration. The contaminant´s molecular composition is uncertain, which might increase the mass calibration error towards larger m/z.

Even though the quantitative measurement of atmospheric analytes present in both gas and particle phase is challenging, the advantages of FIGAERO-CIMS as a semi-quantitative technique, as deployed, are undoubted and for that reason this study was focused on semi-quantitative measurement of atmospheric relevant compounds.

S6 – Comparison between compositions measured by FIGAERO-CIMS, LC-QToF-MS and GC-QToF-MS

For the two major analyte groups, o-MT and o-SQT, we explored the most important compositions from the off-line LC-QToF-MS and GC-QToF-MS results in a similar way as done for the FIGAERO-CIMS results in Fig. 7. The 10 chemical formulas with the highest concentrations for the three different off-line measurements are shown for the time periods covering events A (monoterpene-dominated; Fig. S8) and B (sesquiterpene-dominated; Fig. S9). Most of the chemical formulas that made the top 10 in FIGAERO-CIMS (indicated by blue rectangles in Figs. S8 and S9) were also present among the respective top 10 in LC-QToF-MS, when performed in negative mode (8-9 of 10). This result indicates that, even though LC-QToF-MS has a higher resolution than the used CIMS, the CIMS resolution was likely sufficient for the proper identification of the most important chemical formulas.

Several of the chemical formulas dominating the FIGAERO-CIMS measurements were also present in the positive ionization LC-QToF-MS measurements, whereas just a few were measured by GC-QToF-MS. During the monoterpene event, 5 o-SQT and 6 o-MT that dominated FIGAERO-CIMS measurements were also present in the top 10 chemical formulas measured by positive ionization LC-QToF-MS, but just 2 o-SQT were prevailing in the GC-QToF-MS measurements. Similarly, during the

sesquiterpene event, 4 o-MT and o-SQT were also dominating positive ionization LC-QToF-MS measurements, while only 1 of each chemical formula was present in the GC-QToF-MS top 10. For both LC-QToF-MS (positive mode) and GC-QToF-MS (negative mode) measurements, the most dominant compounds (present in the previous referred top 10) unidentified by CIMS tend to have low H:C ratios. This result suggests that compounds underestimated, or missing, in the FIGAERO-CIMS results included aromatic compounds. One possible explanation for the practical absence of low H:C compounds in CIMS measurements could be related to a higher sensitivity of CIMS for aliphatic compounds in comparison to their aromatic analogues, which would be likely associated with the decrease in polarity of aromatics. The dependence of instrument sensitivity on the polarity of the analytes has been described in previous studies (e.g. Lopez-Hilfiker et al., 2016). The possible thermal decomposition of compounds in FIGAERO-CIMS measurements may also affect the comparability with the other techniques, even though GC-QToF-MS also applies heat during the introduction of the sample into the analytical instrument and high temperatures are applied during ionization for LC-QToF-MS (see Sect. S3). Additional laboratory SOA studies could be helpful to investigate those possibilities, for example such that the same set of instruments is used but with off-line analysis being allowed immediately.

References

Krieger, U. K., Siegrist, F., Marcolli, C., Emanuelsson, E. U., Gøbel, F. M., Bilde, M., Marsh, A., Reid, J. P., Huisman, A. J., Riipinen, I., Hyttinen, N., Myllys, N., Kurtén, T., Bannan, T., Percival, C. J. and Topping, D.: A reference data set for validating vapor pressure measurement techniques: homologous series of polyethylene glycols, Atmos. Meas. Tech., 11(1), 49–63, doi:10.5194/amt-11-49-2018, 2018.

Lee, B. H., Lopez-Hilfiker, F. D., Mohr, C., Kurtén, T., Worsnop, D. R. and Thornton, J. A.: An iodide-adduct high-resolution time-of-flight chemical-ionization mass spectrometer: Application to atmospheric inorganic and organic compounds, Environ. Sci. Technol., 48(11), 6309–6317, doi:10.1021/es500362a, 2014.

Lopez-Hilfiker, F. D., Iyer, S., Mohr, C., Lee, B. H., D'Ambro, E. L., Kurtén, T. and Thornton, J. A.: Constraining the sensitivity of iodide adduct chemical ionization mass spectrometry to multifunctional organic molecules using the collision limit and thermodynamic stability of iodide ion adducts, Atmos. Meas. Tech., 9(4), 1505–1512, doi:10.5194/amt-9-1505-2016, 2016.

Ylisirniö, A., Barreira, L., Pullinen, I., Buchholz, A., Jayne, J., Krechmer, J. E., Worsnop, D. R., Virtanen, A. and Schobesberger, S.: On the calibration of FIGAERO-ToF-CIMS: importance and impact of calibrant delivery for the particle phase calibration, Atmos. Chem. Phys. Discuss., 1–24, doi:10.5194/amt-2020-254, 2020.